ISSN 1063-7842, Technical Physics, 2019, Vol. 64, No. 12, pp. 1808–1813. © Pleiades Publishing, Ltd., 2019.
Russian Text © The Author(s), 2019, published in Zhurnal Tekhnicheskoi Fiziki, 2019, Vol. 89, No. 12, pp. 1902–1908.

PHYSICAL MATERIALS SCIENCE

Influence of the Preparation Method on Amorphous-Crystalline Transition in $Fe_{84}B_{16}$ Alloy

D. Yu. Kovalev[a,*], N. F. Shkodich[a], S. G. Vadchenko[a], A. S. Rogachev[a], and A. S. Aronin[b]

[a] *Merzhanov Institute of Structural Macrokinetics and Materials Science, Russian Academy of Sciences, Chernogolovka, 142432 Russia*

[b] *Institute of Solid State Physics, Russian Academy of Sciences, Chernogolovka, 142432 Russia*

**e-mail: kovalev@ism.ac.ru*

Received September 1, 2018; revised September 1, 2018; accepted June 29, 2019

Abstract—The amorphous-crystalline transition in $Fe_{84}B_{16}$ alloys prepared by melt spinning and high-energy ball milling was studied. Time-resolved X-ray diffraction showed that the kinetics of transition into a crystalline state depends on the method of preparing a metastable alloy. In amorphous $Fe_{84}B_{16}$ alloy prepared by melt spinning, crystallization proceeded within a time period of below 1 s and was accompanied by the formation of eutectic α-Fe–Fe_3B. At temperatures above 600°C, metastable phase Fe_3B was found to transform into Fe_2B and α-Fe. In the high-energy ball milling produced alloy, structural changes were accomplished in 4–8 s and the transition into a state with a perfect crystalline structure was caused by the growth of nanocrystallites formed during processing.

DOI: 10.1134/S1063784219120119

INTRODUCTION

Iron-based amorphous alloys (AAs) showing high magnetic permeability, saturation induction, and low coercive force are used to manufacture magnetic screens, magnetic filters, separators, sensors, etc. [1]. The main method of their preparation is high-speed cooling of the melt using a rotating drum or disk (spinning), which requires high-tech equipment. AAs can be produced by high-energy ball milling (HEBM) [2–5]. To obtain materials with necessary magnetic properties, the AAs should be partially crystallized in optimal annealing conditions [6]. Crystallization occurring upon heating of AAs changes their physicomechanical properties. In this case, there is a problem of thermal stability. The crystallization of tapes of an amorphous $Fe_{84}B_{16}$ alloy prepared by spinning was studied in [7–10]. It was shown that amorphous-crystalline transition during slow heating occurs in two stages. In the first stage, the α-Fe phase is formed; in the second one, metastable phase Fe_3B precipitates, which decomposes into α-Fe and Fe_2B with increasing temperature. The study of amorphous tapes [11] showed that wave-like crystallization can be initiated by a coil heated at $T_0 = 300$°C. The amorphous tapes with similar composition ($Fe_{80}B_{20}$) undergo no crystallization upon heating at a rate of 20 K/min to 420°C or during isothermal annealing at 380°C for 1 h [12]. However, there are no studies on the processes occurring during heating of tapes produced by rolling of AA powders. This study is aimed at studying the transition of amorphous $Fe_{84}B_{16}$ alloy produced by HEBM into a crystalline state by time-resolved dynamic X-ray diffraction analysis with special emphasis on crystallization of amorphous tapes prepared by melt spinning.

EXPERIMENTAL

Iron (OSCh 6-2 grade, TU 6-09-3000-78) and amorphous boron (B-99V grade, TU 1-92-154-90) powders were used as the starting components to produce $Fe_{84}B_{16}$ alloy by HEBM. The powders were mixed in a Fe : B ratio of 84 : 16 at % in a porcelain mortar for 5–10 min. The components were weighed using an VM2202M-II electronic laboratory balance with an accuracy of at least 0.01 g.

HEBM of powder mixtures 84Fe : 16B was carried out in an Activator-2S laboratory planetary ball mill at a planetary disk rotation speed of 700 rpm and a drum rotation speed of 1400 rpm. The pre-mixed 84Fe : 16B charge and steel balls 7–8 mm in diameter were placed into the activator drums in a weight ratio of 20 : 1 (360 g balls per 18 g mixture). The mill drums were hermetically closed using caps with valves for pumping and inflowing gas. The drums were evacuated to a residual pressure of 0.01 Pa and then filled with argon up to 4 atm. The 84Fe : 16B mixture was subjected to high energy ball milling for up to 120 min. The pro-

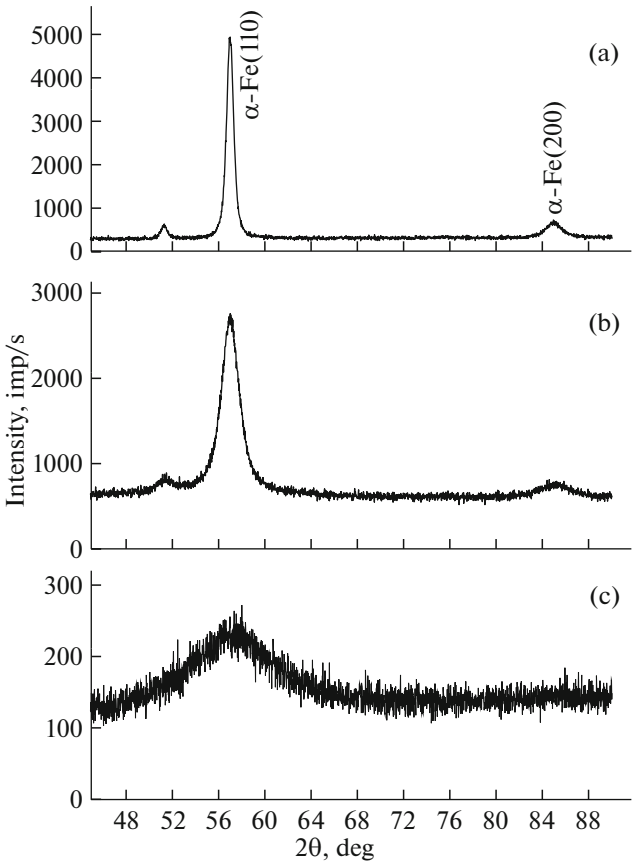

Fig. 1. XRD patterns of (a) Fe powder after mechanical treatment, (b) 84Fe : 16B mixture after mechanical treatment, and of (c) 84Fe16B AA prepared by spinning.

duced powders were rolled into tapes 250–300 μm thick and 12 mm wide.

The sequence of structural and phase transformations was studied by time-resolved X-ray diffraction (TRXRD) analysis, which makes it possible in situ to detect changes in the structural and phase states of the material upon heating [13]. The idea of TRXRD is sequence recording of X-ray diffraction patterns with short exposure time during heating. The TRXRD studies were performed using monochromatic copper radiation ($\lambda = 0.154187$ nm) in the Bragg–Brentano reflection geometry. The foil made of 84Fe16B AA prepared by melt spinning with a thickness of 30 μm [14] and the rolled tape fabricated from HEBM-produced 84Fe : 16B powder mixture with a thickness of 200 μm were studied. A part of foil or band 15 × 10 mm in size was placed in a hermetic chamber equipped with a resistance furnace and beryllium windows. The monochromatic beam was directed onto the center of the sample surface at an angle of 20°; the illuminated area was 2 × 10 mm in size. XRD patterns were recorded continuously during heating. The exposure time of an XRD pattern for foil and tape was 1 and 2 s, respectively. Several series consisting of 64 XRD pat-

Table 1. α-Fe cell parameters

Sample	α-Fe cell parameter, Å	Crystalline phases
Fe, after HEBM	2.8664	α-Fe
84Fe–16B after HEBM	2.8683	α-Fe
84Fe–16B after HEBM and heating to 460°C	2.8674	α-Fe
Amorphous 84Fe16B alloy after heating at 460°C	2.8681	α-Fe, Fe_2B
Amorphous 84Fe16B alloy after heating at 8000°C	2.8681	α-Fe, Fe_2B
Fe, PDF card no. 06-0696	2.8664	α-Fe

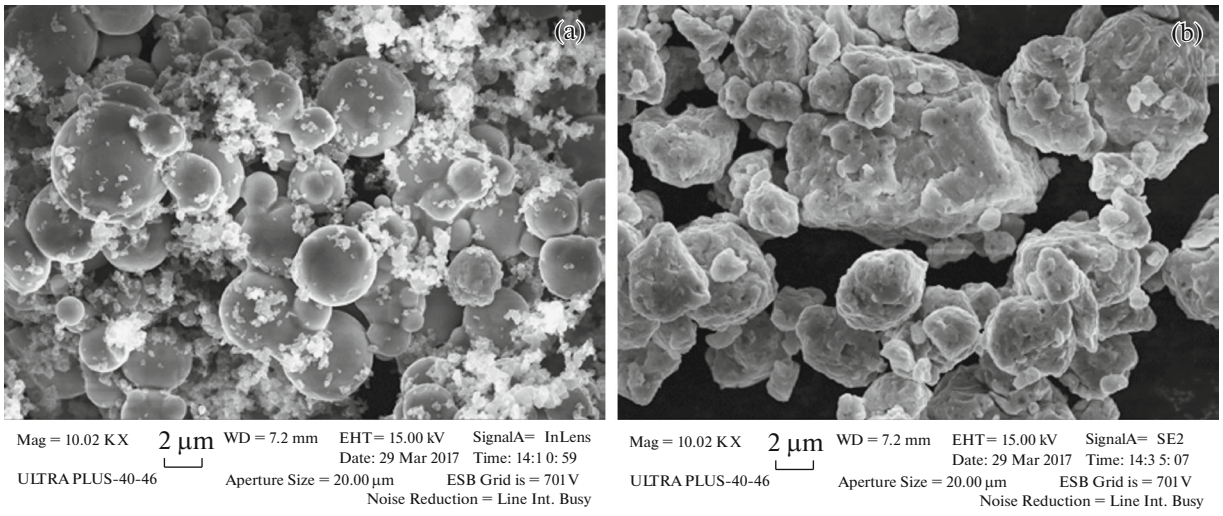

Fig. 2. SEM images of the 84Fe : 16B powder mixture (a) before and (b) after HEBM for 80 min.

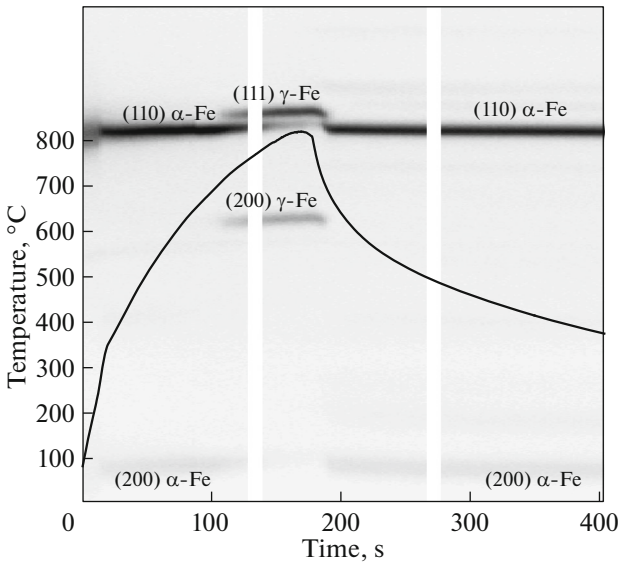

Fig. 3. TRXRD pattern taken during heating of HEBM-produced 84Fe : 16B powder mixture.

terns were obtained during heating and cooling of the sample. The temperature was measured using a VR 5/20 thermocouple 100 μm in diameter the junction of which was in contact with the surface of the sample. The heating rate was 250–280 deg/min. The experiments were carried out in a helium atmosphere under an excess pressure of 1 atm.

X-ray diffraction (XRD) analysis of the material before and after crystallization was carried out using a DRON-3M diffractometer with FeK_α radiation in the step-by-step scanning mode and in the range of angles $2\theta = 30°–100°$ with a step of 0.02° and holding for 2 s. The cell parameters were determined by the internal standard method using Si standard (SRM 640D). The fine structure parameters were estimated by the second moment method using the Size & Strain software package (NPP Burevestnik) and LaB_6 (SRM 660A) was used as a standard reference material.

RESULTS AND DISCUSSION

XRD analysis showed that the 84Fe : 16B powder mixture after mechanical treatment is not amorphous (Fig. 1b). The XRD pattern contains strongly broadened lines of bcc α-Fe phase (PDF card no. 06-0696), which are typical of (110) and (200) for K_α series and (110) for K_β series. The size of α-Fe coherent domains was 9 nm. Figure 2 shows SEM images of the powder mixture before and after HEBM. HEBM is seen to yield composite particles 2–10 μm in size. The α-Fe phase cell parameter $a = 2.8683$ Å is higher than the known value of the Fe cell parameter in the ICDD powder database (see Table 1).

In order to explain the reasons of change in the α-Fe cell size, the ball milling of pure α-Fe powder was carried out in the same conditions of mechanical treatment. In this case, the broadening of α diffraction

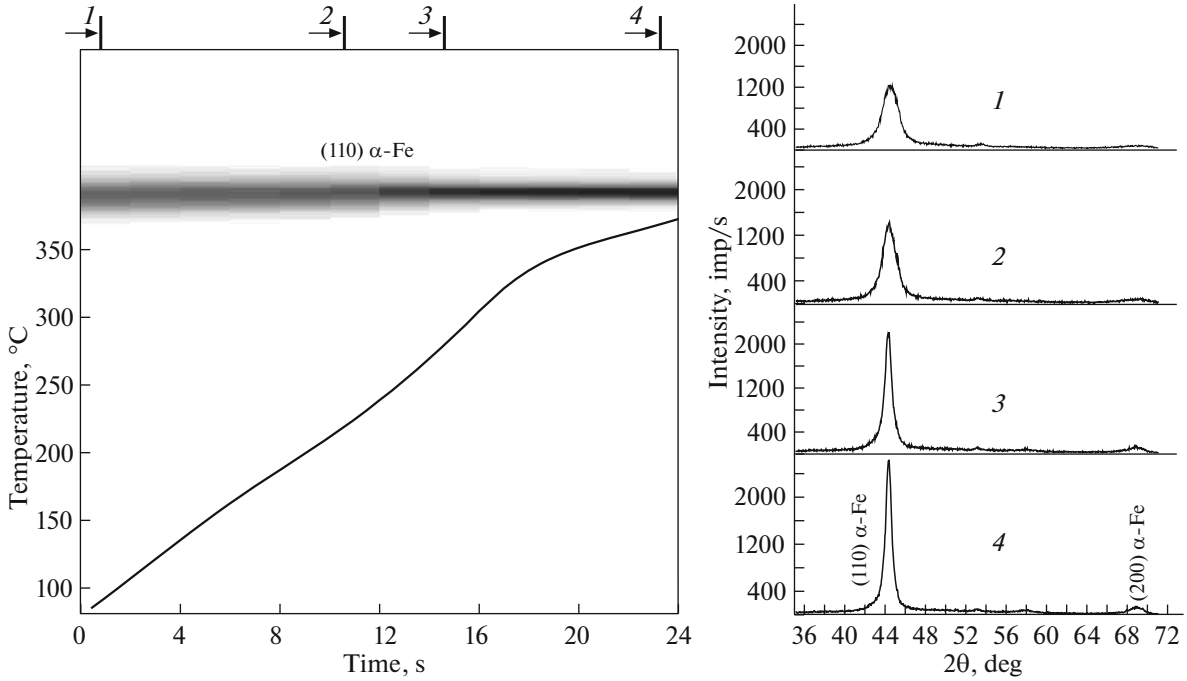

Fig. 4. Initial part of TRXRD pattern taken during heating of HEBM-produced 84Fe : 16B powder mixture.

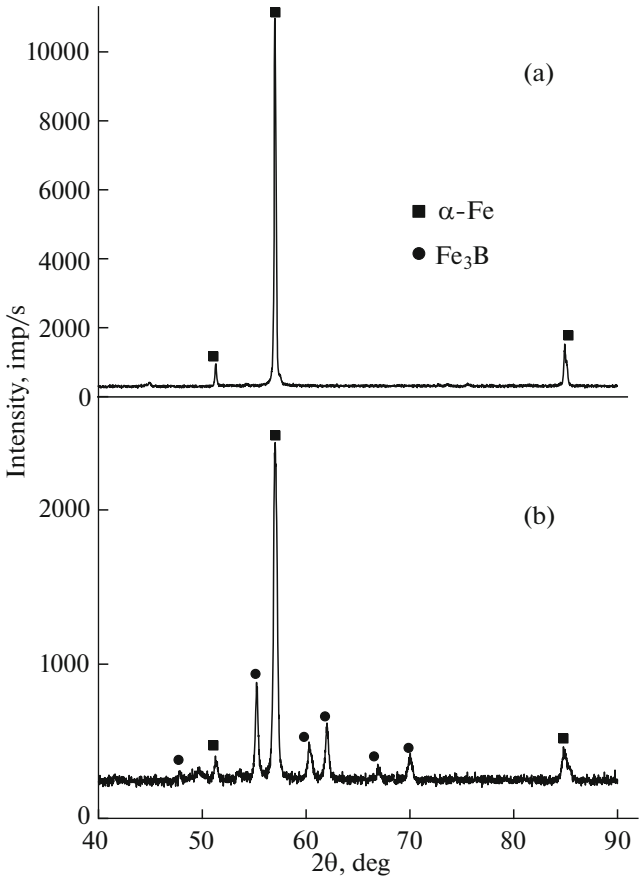

Fig. 5. XRD patterns of (a) HEBM-produced 84Fe : 16B after heating at 820°C, and (b) 84Fe16B AA after heating at 460°C.

lines is substantially less (Fig. 1a); cell parameter a = 2.8664 Å corresponds to the database value. Therefore, high-energy processing does not lead to a change in the unit cell size of α-Fe. Thus, structural changes are influenced by the second component (boron). The equilibrium Fe–B phase diagram shows that the solubility of boron in α-Fe is insignificant and is no more than 0.06 at % at room temperature [15]. It is known that mechanical activation favors a significant shift of concentration boundaries of solid solutions beyond the equilibrium state [16]. Thus, HEBM of the 84Fe : 16B mixture leads to the formation of metastable solid solution of boron in α-Fe and, accordingly, to an increase in the α-Fe cell parameter (see Table 1). The observed difference in the broadening of α-Fe diffraction lines (Figs. 1a, 1b) also indicates the effect of boron on the structure of the material. The issue of concentration of boron in the α-Fe solid solution, which was formed as a result of treatment of the 84Fe : 16B mixture, requires further studies. Complete dissolution of 16 at % B in α-Fe is unlikely. It can be assumed that the obtained composite particles contain nanosized crystalline regions of the α-Fe [B] solid solution separated by regions of amorphous boron.

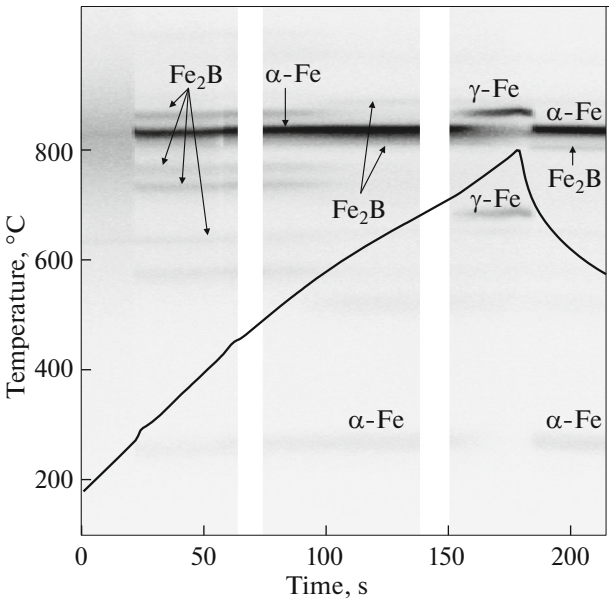

Fig. 6. TRXRD pattern taken during heating of amorphous 84Fe16B alloy.

The $Fe_{84}B_{16}$ alloy prepared by melt spinning is amorphous. This was confirmed by a diffuse line presented in the XRD pattern (Fig. 1c). $Fe_{84}B_{16}$ alloy was widely studied in [7–10, 17, 18]. Its crystallization during slow heating (~20 deg/min) was found to proceed in several stages. At the first stage, the equilibrium bulk centered α-Fe phase precipitates. Then, the metastable tetragonal Fe_3B phase is formed. At higher temperatures, the Fe_3B phase converts to stable crystalline α-Fe and Fe_2B phases. Figure 3 shows the TRXRD pattern and heating thermogram of HEBM-produced 84Fe : 16B powder. A sequence of 192 XRD patterns acquired every 2 s is presented in a two-dimensional field with coordinates (angle, time).

Figure 4 shows that only crystalline α-Fe phase is formed upon heating of the 84Fe : 16B mixture. An increase in the intensity and a narrowing of α-Fe lines broadened as a result of HEBM start at 250–300°C within 4–6 s. An increase in the degree of crystallinity of α-Fe is accompanied by the appearance of a weakly expressed exothermic peak in the thermogram. The presence of thermal peak is associated with the release of energy during the transition into an equilibrium state. Further heating at a temperature of more than about 700°C favors the α-Fe → γ-Fe phase transition (Fig. 3). At 820°C, there are lines belonging to the face-centered γ-Fe phase in the diffraction field. The reverse transition upon cooling occurs at the same temperature (about 700°C). For comparison, the evolution of the structure of pure α-Fe powder fabricated by HEBM was studied upon heating to 850°C. It was found that the α-Fe phase is stable and does not undergo structural transformations in this tempera-

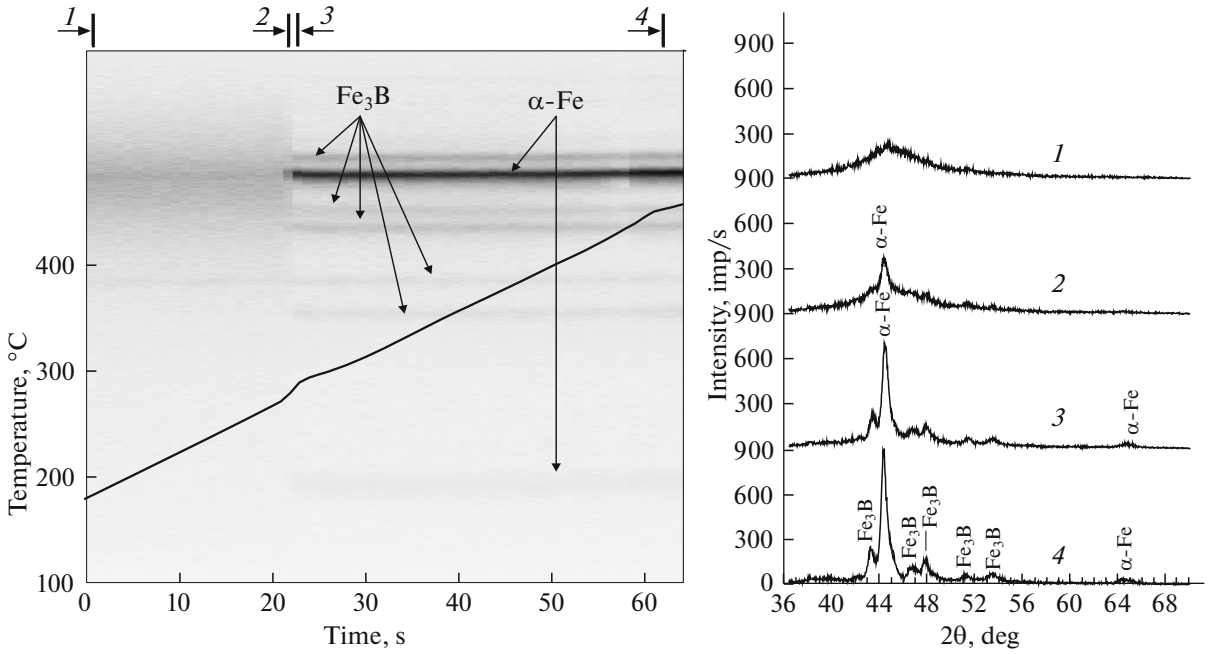

Fig. 7. Initial part of TRXRD pattern taken during heating of amorphous 84Fe16B alloy.

ture range. Indeed, the polymorphic α-Fe ↔ γ-Fe transformation takes place at 912°C. Obviously, a significant decrease in the transition temperature is associated with dissolution of boron, which is a stabilizer of the austenitic phase. The XRD pattern after cooling is seen in Fig. 5a to contain only α-Fe phase. The cell parameter of the α-Fe phase after heating is less than that of the α-Fe phase after HEBM, however, it remained above the known values of the PDF 2 database (see Table 1). Thus, the results confirm the formation of solid solution of boron in α-Fe during HEBM of the 84Fe : 16B mixture. Upon heating, the boron concentration in α-Fe decreases as indicted by a decrease in the cell size. No crystalline boride phases of iron are formed at given experimental temperature and time parameters.

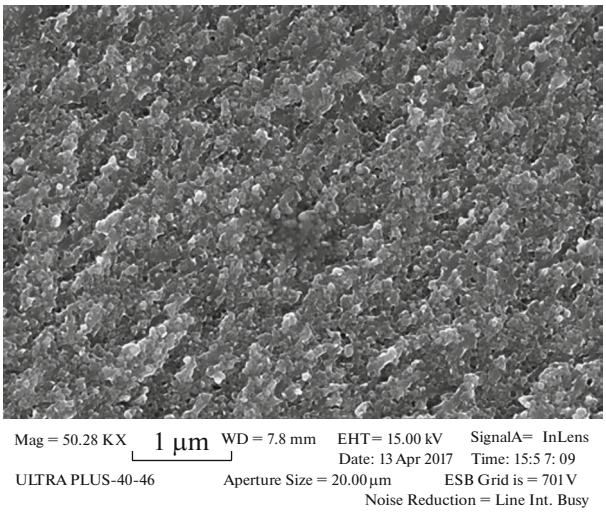

Fig. 8. Microstructure of amorphous 84Fe16B alloy after heating at 460°C.

Figure 6 shows the TRXRD pattern taken upon heating of amorphous $Fe_{84}B_{16}$ alloy and consisting of 192 diffraction patterns acquired every 1 s.

The amorphous-crystalline transition of the $Fe_{84}B_{16}$ alloy prepared by spinning occurs within a time period of below 1 s. At the heating rate of 250–280 deg/min, α-Fe and Fe_3B phases are crystallized simultaneously (Fig. 7). This is indicated by the thermal effect in the thermogram. The $Fe_{84}B_{16}$ alloy has a eutectic composition and is crystallized by the eutectic mechanism, forming colonies 50–100 nm in size (Fig. 8). The XRD pattern of the alloy after heating to 460°C contains two phases: α-Fe and Fe_3B (Fig. 5b).

The cell parameter of α-Fe in the sample heated to 460°C, $a = 2.8683$ Å exceeds the corresponding value for pure α-Fe ($a = 2.8664$ Å, see Table 1), which indicates the formation of a solid solution of boron in α-Fe. It should be noted that the sizes of α-Fe cells produced by HEBM, α-Fe with B, and α-Fe precipitating during crystallization of $Fe_{84}B_{16}$ AA, are close to each other. Above 600°C, the signals from metastable phase Fe_3B disappear, while the lines of the Fe_2B phase come into being (PDF card no. 36-1332). Further heating leads to α-Fe → γ-Fe phase transition (Fig. 6). The onset of polymorphic transformation is around about 700°C just as in the case of heating of HEBM-produced powder. During cooling, the

reverse transition γ-Fe → α-Fe is observed. The cell parameter of α-Fe in the $Fe_{84}B_{16}$ alloy after heating to 800°C is less than that in the alloy heated to 460°C, however, it remained above the cell parameter of pure α-Fe (see Table 1).

The evolution of the structure and phase composition of amorphous and HEBM-produced $Fe_{84}B_{16}$ alloys during heating differs, which is caused by different methods of synthesis. Heating of amorphous $Fe_{84}B_{16}$ alloy allows obtaining a eutectic α-Fe–Fe_3B nanostructure. In case of heating of an HEBM-produced 84Fe : 16B powder mixture, there are no iron boride phases; a gradual transition of α-Fe nanostructure in the equilibrium state with perfect crystalline structure occurs. Composite particles contain nanoscale ferrite regions (about 9 nm), which are nuclei for crystalline α-Fe grains. The onset of crystallization (250–300°C) is close to $0.2–0.3T_{melt}$, at which diffusion-controlled normal grain growth in metals starts. The crystallization is diffusion-controlled and accomplished in 4–8 s. The crystallization of amorphous $Fe_{84}B_{16}$ alloy is explosive in its character and is associated with simultaneous formation of nanoscale crystalline regions in the entire bulk of the material, i.e., with a high rate of formation of nuclei in the amorphous matrix.

CONCLUSIONS

Time-resolved X-ray diffraction method was applied to exploring amorphous-crystalline transition in $Fe_{84}B_{16}$ alloys prepared by spinning and high-energy ball milling. It is shown that the kinetics of transition into a crystalline state is determined by the method of preparation of metastable alloy.

HEBM of the 84Fe : 16B powder mixture yields composite particles consisting of nanoscale crystalline regions of α-Fe [B] solid solution and regions of amorphous boron. Heating of this powder mixture favors no formation of iron boride phases but is accompanied by a gradual transition of a nanostructure of α-Fe in the equilibrium state with perfect crystalline structure. The transition into crystalline state is induced by diffusion and is caused by the growth of nanocrystallites formed during HEBM as the nuclei for crystal α-Fe grains.

Upon heating of amorphous $Fe_{84}B_{16}$ alloy prepared by melt spinning, a eutectic α-Fe–Fe_3B nanostructure is formed. The crystallization of $Fe_{84}B_{16}$ AA is explosive in its character and is associated with simultaneous formation of nanoscale crystalline regions over the entire bulk of the material, i.e., with a high rate of formation of nuclei in amorphous matrix.

FUNDING

The work was supported by the State-supported research program for the Institute of Structural Macrokinetics and Materials Science, Russian Academy of Sciences (no. 44.1).

CONFLICT OF INTEREST

The authors declare that they do not have any conflicts of interest.

REFERENCES

1. B. Zhang, W. Hu, and D. Zhu, Phys. B **183**, 205 (1993).
2. C. Politis, Int. J. Mod. Phys. B **22**, 2905 (2008).
3. A. Calka and A. P. Radlinski, Appl. Phys. Lett. **58**, 119 (1991).
4. N. F. Shkodich, S. G. Vadchenko, A. A. Nepapushev, D. Yu. Kovalev, I. D. Kovalev, S. Ruvimov, A. S. Rogachev, and A. S. Mukasyan, J. Alloys Compd. **741**, 575 (2018).
5. T. F. Grigor'eva, A. P. Barinova, and N. Z. Lyakhov, *Mechanochemical Synthesis in Metallic Systems* (Parallel', Novosibirsk, 2008).
6. T. Kulik, J. Non-Cryst. Solids **287**, 145 (2001).
7. T. Nakajima, E. Kita, and H. Ino, J. Jpn. Inst. Met. Mater. **51**, 263 (1987).
8. M. W. Ruckman, R. A. Levy, A. Kessler, and R. J. Hasegama, J. Non-Cryst. Solids **40**, 393 (1980).
9. A. A. Novakova and T. Yu. Kiseleva, Vestn. Mosk. Univ. Fiz. Astron. **36**, 56 (1995).
10. A. A. Novakova, T. Yu. Kiseleva, and I. A. Aleksandrova, Vestn. Mosk. Univ. Fiz. Astron. **35**, 102 (1994).
11. A. S. Rogachev, S. G. Vadchenko, A. S. Aronin, S. Rouvimov, A. A. Nepapushev, I. D. Kovalev, F. Baras, O. Politano, S. A. Rogachev, and A. S. Mukasyan, Appl. Phys. Lett. **111**, 093105 (2017).
12. G. E. Abrosimova, A. S. Aronin, S. V. Dobatkin, I. I. Zver'kova, D. V. Matveev, O. G. Rybchenko, and E. V. Tat'yanin, Phys. Solid State **49**, 1034 (2007).
13. D. Yu. Kovalev and V. I. Ponomarev, Int. J. Self-Propag. High-Temp. Synth. **28**, 114 (2019).
14. K. Suzuki, H. Fujimori, and K. Hashimoto, *Amorphous Metals*, Ed. by S. Masumoto (Metallurgiya, Moscow, 1987).
15. K. I. Portnoi, M. Kh. Levinskaya, and V. M. Romashov, Poroshk. Metall., No. 8, 66 (1969).
16. V. V. Boldyrev, in *Fundamentals of Mechanical Activation, Mechanosynthesis, and Mechanochemical Technology*, Ed. by E. G. Avvakumov (Sib. Otd. Ross. Akad. Nauk, Novosibirsk, 2009), p. 15.
17. U. Herold and U. Koster, Z. Metallkd. **69**, 326 (1978).
18. G. E. Abrosimova and A. S. Aronin, Int. J. Rapid Solidif. **6**, 29 (1991).

Translated by O. Golosova